

# Relative stabilities of Ce(IV) and Ce(III) limiting carbonate complexes at 5–50 °C in Na<sup>+</sup> aqueous solutions, an electrochemical study

Nathalie Larabi-Gruet<sup>a,\*</sup>, Annie Chaussé<sup>a,\*\*</sup>, Ludovic Legrand<sup>a</sup>, Pierre Vitorge<sup>a,b</sup>

<sup>a</sup> Laboratoire Analyse et Modélisation pour la Biologie et l'Environnement (CNRS-CEA-Université d'Evry UMR 8587),

Université d'Evry Val d'Essonne, 1 rue du Père Jarlan, 91025 Evry Cedex, France

<sup>b</sup> CEA-Saclay, DEN/DPC/SECR/LSRM, 91191 Gif-sur-Yvette Cedex, France

Received 4 May 2006; received in revised form 10 August 2006; accepted 23 August 2006

Available online 26 September 2006

## Abstract

The normal potential of the Ce(IV)/Ce(III) redox couple was determined by square wave voltammetry (SWV) at different temperatures in solutions with a constant ratio  $[\text{CO}_3^{2-}]/[\text{HCO}_3^-] \approx 10$  for high ionic strengths (3.29 mol dm<sup>-3</sup> at 4.39 mol dm<sup>-3</sup>):  $E_{\text{IV/III}}^0$  varies from 259.5 to 198.0 mV/S.H.E. in the 15–50 °C range. Linear variations were found for  $E_{\text{IV/III}}^0$  versus  $(RT/F)\ln(m_{\text{CO}_3^{2-}})$ , leading to the stoichiometry, Ce(CO<sub>3</sub>)<sub>6</sub><sup>8-</sup> for the Ce(IV) limiting complex. But the slopes of these linear variations were actually found in the range 1.8–1.9, not exactly 2. This was interpreted as dissociation of the Ce(IV) limiting complex following the reaction: Ce(CO<sub>3</sub>)<sub>5</sub><sup>6-</sup> + CO<sub>3</sub><sup>2-</sup> → Ce(CO<sub>3</sub>)<sub>6</sub><sup>8-</sup> and as dissociation of the Ce(III) limiting complex following the reaction: Ce(CO<sub>3</sub>)<sub>3</sub><sup>3-</sup> + CO<sub>3</sub><sup>2-</sup> → Ce(CO<sub>3</sub>)<sub>4</sub><sup>5-</sup>; for which maximum possible values of log<sub>10</sub>  $K_{\text{IV},6}$  and log<sub>10</sub>  $K_{\text{III},4}$  were estimated via fitting in the 15–50 °C temperature range (log<sub>10</sub>  $K_{\text{IV},6}$  = 0.42 (0.97) and log<sub>10</sub>  $K_{\text{III},4}$  = 0.88 (7.00) at 15 °C (50 °C). The normal potential was found to decrease linearly with  $T$ , these variations correspond to  $T^0 \Delta_r S_{70} \approx -46 \text{ kJ mol}^{-1}$ , with  $T^0 = 298.15 \text{ K}$  and  $\Delta_r H_{70} \approx -70 \text{ kJ mol}^{-1}$ . The apparent diffusion coefficient of Ce(IV) was determined by direct current polarography (DCP), cyclic voltammetry (CV) and square wave voltammetry. It was found to depend on the ionic strength and to be proportional to  $T$ .

© 2006 Elsevier Ltd. All rights reserved.

**Keywords:** Cerium; Carbonate complexes; Square wave voltammetry; Temperature dependence; Thermodynamic constants

## 1. Introduction

In the framework of high-level radioactive waste underground repositories, safety assessments require to evaluate radiotoxicity induced by the possible release of radionuclides into natural aquifers [1]. Migration of radionuclides is either limited by their solubilities and interactions with inorganic materials (i.e., via co precipitation or/and sorption) or increased by complexation with inorganic or organic ligands present in groundwater. So, in this context, considerable efforts have been made in the past 20 years to construct reliable thermodynamic databases regarding the chemistry of long-lived radionuclides to assess their release from waste repositories into environmental waters: see the reviews for the thermochemical database (TDB) of the OECD NEA (Organ-

isation for Economic Co-operation and Development, Nuclear Energy Agency) on U [2], Am [3], Tc [4], Np [5] and Pu [5] and their recent update [6].

Because of their important roles in groundwater, complexation reactions of typically actinides(III) and (IV) or their lanthanide analogues with carbonate have been the focus of major attention. Studies were done using high carbonate concentrations in order to obtain the limiting carbonate complexes, thereby avoiding mixtures of too many species that might have altered the selectivity of the technique. Techniques used for investigating the stoichiometries and the stability of the carbonate complexes are numerous: time-resolved laser-induced fluorescence spectroscopy (Cm(CO<sub>3</sub>)<sub>3</sub><sup>3-</sup> and Am(CO<sub>3</sub>)<sub>3</sub><sup>3-</sup> in [7]), solubility measurements (Eu(CO<sub>3</sub>)<sub>3</sub><sup>3-</sup> in [8]), electrochemical techniques (the Am(IV)/Am(III) couple in [9] and the Ce(IV)/Ce(III) couple in [10]). These last techniques can be used only when the couples have an electrochemical reversible behaviour.

Studies have already been devoted to the limiting carbonate complexes of cerium, an analogue of actinide at temperatures close to ambient. In [11], Ferri et al. suggested the stoichiom-

\* Corresponding author. Tel.: +33 1 69477703; fax: +33 1 69477655.

\*\* Corresponding author. Tel.: +33 1 69477707.

E-mail addresses: [nathalie.gruet@univ-evry.fr](mailto:nathalie.gruet@univ-evry.fr) (N. Larabi-Gruet), [annie.chausse@univ-evry.fr](mailto:annie.chausse@univ-evry.fr) (A. Chaussé).

etry,  $\text{Ce}(\text{CO}_3)_4^{5-}$  for the Ce(III) limiting carbonate complex when  $[\text{CO}_3^{2-}] > 1 \text{ mol dm}^{-3}$ ; a dissociation of this species into  $\text{Ce}(\text{CO}_3)_3^{3-}$  was also considered in this study. Dervin and Faucherre [12,13] proposed the two following Ce(IV) carbonate complexes,  $\text{Ce}(\text{CO}_3)_6^{8-}$  and  $\text{Ce}(\text{CO}_3)_5^{6-}$  depending on the  $\text{CO}_3^{2-}$  concentration range. A recent electrochemical study [10] confirmed the nature of the limiting complexes of Ce(IV) and Ce(III), ( $\text{Ce}(\text{CO}_3)_6^{8-}$  and  $\text{Ce}(\text{CO}_3)_4^{5-}$ ). An UV/visible absorption spectroscopy study [14] suggested the dominant species,  $\text{Ce}(\text{CO}_3)_5^{6-}$  in dilute carbonate solution. Knowledge of the stoichiometry of the limiting complexes is very important because they can be starting points to determine aqueous speciation in environmental conditions. This way allows omitting no species in the speciation that could affect the numerical values of the stability constants fitted for the other complexes.

Currently, a few studies on the M(IV)/M(III) couple behaviour (where M = lanthanide and actinide) with the temperature in concentrated carbonate/bicarbonate media were carried out. Consequently, there is a few available information in this field in the thermodynamic and chemical data bank whereas it is well established that the radioactive decays would increase the temperature in the vicinity of the waste packages, in the early stage of the disposal, inducing modifications in the aqueous speciation. It should be noticed that one study relative to the hydrolysis reaction of Ce(IV) in perchloric acid solution is given in [15]; a  $\ln K - T$  linear relationship was found allowing the determination of the reaction entropy  $\Delta_r S$  and enthalpy  $\Delta_r H$ .

The first aim of our study concerns the nature of the Ce(IV) limiting carbonate complex because the stoichiometry,  $\text{Ce}(\text{CO}_3)_6^{8-}$ , is still under discussion; indeed, it differs from that reported for U and trans U limiting complexes in carbonate solutions. Our approach consists in deducing the complex formula from the carbonate loss when going from the carbonate complex of Ce(IV) to that of Ce(III) using the square wave voltammetry (SWV). The validity of this approach is based on the reversibility of the Ce(IV)/Ce(III) couple that was verified in the present study. The second aim of our study concerns the influence of the temperature on the Ce limiting carbonate complexes (stoichiometry and dissociation). Electrochemical data relative to the Ce(IV)/Ce(III) couple enables us also to deduce from their variations with the temperature: the thermodynamic constants,  $K_{\text{IV},6}$  and  $K_{\text{III},4}$  of equilibria:  $\text{Ce}(\text{CO}_3)_5^{6-} + \text{CO}_3^{2-} \rightleftharpoons \text{Ce}(\text{CO}_3)_6^{8-}$  and  $\text{Ce}(\text{CO}_3)_3^{3-} + \text{CO}_3^{2-} \rightleftharpoons \text{Ce}(\text{CO}_3)_4^{5-}$ , the entropy  $\Delta_r S_{T^0}$  and the enthalpy  $\Delta_r H_{T^0}$ .

## 2. Experimental details

The test solutions were prepared with  $\text{Ce}(\text{SO}_4)_2 \cdot 4\text{H}_2\text{O}$  ( $\geq 98.0\%$ ) from VWR. All the other reagents were of analytical grade purity from Sigma–Aldrich. The solutions were prepared with  $18 \text{ M}\Omega \text{ cm}$  nano-pure water, and deaerated with argon (U, Air Liquide). They were thermostated in the temperature range  $5\text{--}50^\circ\text{C}$  with a Polystat 23 apparatus from Fisher Bioblock Scientific. Freshly prepared Ce(IV) solutions were always used.

All electrochemical measurements were performed using an Autolab pgstat30 potentiostat/galvanostat (Eco Chemie) system controlled by a computer. It was equipped with a Model 663

VA Stand (Metrohm) and its multimode electrode (Metrohm, model 6.1246.020) as working electrode, used in the static mercury drop electrode (SMDE) mode, the radius of the mercury drop was  $1.95 \times 10^{-2} \text{ cm}$ . A glassy carbon wire (6.1247.000, Metrohm) and an Ag/AgCl wire (6.0728.000, Metrohm) were used as auxiliary and reference electrodes, respectively. In order to avoid possible damages of the reference electrode by carbonate ions, the Ag/AgCl wire was isolated from the test solution by means of a capillary extension (6.1245.000, Metrohm) filled of a  $0.02 \text{ mol}\cdot\text{dm}^{-3} \text{ NaCl}$ , ( $I_c$ ,  $-0.02$ )  $\text{mol}\cdot\text{dm}^{-3} \text{ NaClO}_4$  solution of same molar ionic strengths,  $I_c$ , as the test solutions.  $E_{\text{Ref}}(T)$ , the potential of this reference electrode was checked once a week, it was stable within  $2.5 \text{ mV}$ .

The reference electrode potential was calculated from Nernst Law and  $a_{\text{Cl}^-, \text{Ref}}$ , the activity of ion  $\text{Cl}^-$  in the  $\text{NaCl}/\text{NaClO}_4$  aqueous solutions of the capillary extension. The ionic strength of the solution in the capillary extension and that of the test solution are the same for minimizing  $E_j$ , the junction potential. Nevertheless,  $E_j$  was measured at three temperatures ( $5$ ,  $25$  and  $50^\circ\text{C}$ ) in two test solutions ( $1.00 \text{ mol dm}^{-3} \text{ Na}_2\text{CO}_3/0.10 \text{ mol dm}^{-3} \text{ NaHCO}_3/1.27 \text{ mol dm}^{-3} \text{ NaNO}_3/0.02 \text{ mol dm}^{-3} \text{ NaCl}$  and  $1.42 \text{ mol dm}^{-3} \text{ Na}_2\text{CO}_3/0.13 \text{ mol dm}^{-3} \text{ NaHCO}_3/0.02 \text{ mol dm}^{-3} \text{ NaCl}$ ), where a second Ag/AgCl wire was plunged, i.e. a typical cell for measuring  $E_j$  was  $\text{Ref}||0.02 \text{ mol dm}^{-3} \text{ NaCl} + 1.00 \text{ mol dm}^{-3} \text{ Na}_2\text{CO}_3 + 0.10 \text{ mol dm}^{-3} \text{ NaHCO}_3 + (I_c - 0.02 - 3c_{\text{Na}_2\text{CO}_3} - c_{\text{NaHCO}_3}) \text{ mol dm}^{-3} \text{ NaNO}_3 | \text{Ag}/\text{AgCl}$  wire, where Ref is our usual reference electrode. These two test solutions were chosen because they represent the lower and higher carbonate concentrations used in this work. The lower limit of  $1.00 \text{ mol dm}^{-3} \text{ Na}_2\text{CO}_3$  was chosen because below this concentration,  $\text{Ce}(\text{SO}_4)_2 \cdot 4\text{H}_2\text{O}$  is not soluble. The upper limit of  $1.42 \text{ mol dm}^{-3} \text{ Na}_2\text{CO}_3$  was chosen because it is the maximum solubility of  $\text{Na}_2\text{CO}_3$  at  $5^\circ\text{C}$ . All the test solutions used in this work were pH buffered solutions, thus it was not possible to detect possible differences in the hydroxide speciations between Ce(IV) and Ce(III), only the Ce(IV) and Ce(III) carbonate speciations were studied.

The pH was measured with a Radiometer XC161 combined glass electrode connected to a Tacussel ISIS 20000 pH-meter. The pH combined glass electrode was calibrated with the initial solutions used for the electrochemical measurements, since they were actually  $\text{HCO}_3^-/\text{CO}_3^{2-}$  pH buffers. The speciation of these pH buffers – including  $m_{\text{H}^+}$ , the  $\text{H}^+$  molal concentration – was calculated as outlined below (Section 3), and the electrode was calibrated in  $-\log_{10} m_{\text{H}^+}$  unit and not activity, i.e.  $-\log_{10} a_{\text{H}^+}$ . The electrode was also checked with commercial pH buffers, it appeared that this gave virtually the same calibration for pH (i.e.,  $-\log_{10} a_{\text{H}^+}$ ). This was not especially expected since different junction potential values were expected between both calibrations as a result of differences in ionic strengths, which were accounted for only in activity coefficients—not in junction potentials. Anyhow, pH was only measured for checking: it was not used in the quantitative treatment of our experimental data. After argon bubbling for 30 min, a blank voltamogram was recorded at three temperatures ( $5$ ,  $25$  and  $50^\circ\text{C}$ ) for each carbonate/bicarbonate solution without Ce(IV).

This enables us to check the absence of any electroactive impurities and to verify that the mercury of the working electrode does not form complexes in the presence of high concentrations of carbonate. The normal potential of Ce(IV)/Ce(III) redox couple,  $E_{IV/III}^0(T)$ , was determined by square wave voltammetry and the apparent diffusion coefficient of Ce(IV),  $D_{IV}$ , was determined by square wave voltammetry, cyclic voltammetry (CV) and direct current polarography (DCP).  $E_{IV/III}^0(T)$  and  $D_{IV}$  values are results of 10 electrochemical measurements.

### 3. Treatment of the data

#### 3.1. Electrochemical parameters

An extended presentation of square wave voltammetry was given by different authors [16–22]. The forward and backward individual currents,  $I_f$  and  $I_b$  and the differential current,  $\Delta I$  are given in Fig. 1. The half-height width of a wave,

$$L_{1/2} = r_f T \log_{10} \frac{b + \sqrt{b^2 - \xi}}{b - \sqrt{b^2 - \xi}} \quad (1)$$

where  $r_f = R \ln 10 / F$ ,  $F = 96485.309 \text{ C mol}^{-1}$  is Faraday Constant,  $R = 8.314510 \text{ J K}^{-1} \text{ mol}^{-1}$  is the molar gas constant and with  $b = \xi/2 + 2\sqrt{\xi} + 1/2$  and  $\xi = \exp(F|E_{sw}|/RT)$ , is a good criteria to check the reversibility of a redox system. Another criteria of reversibility is the purchase of two symmetrical waves with respect to the potential axis in the reductive and oxidative directions [23]. In our experiments, with solutions containing only Ce(IV) (oxidant species), SWV measurements were done as follows: a reductive direction was performed in the negative direction, starting at a potential where the concentration

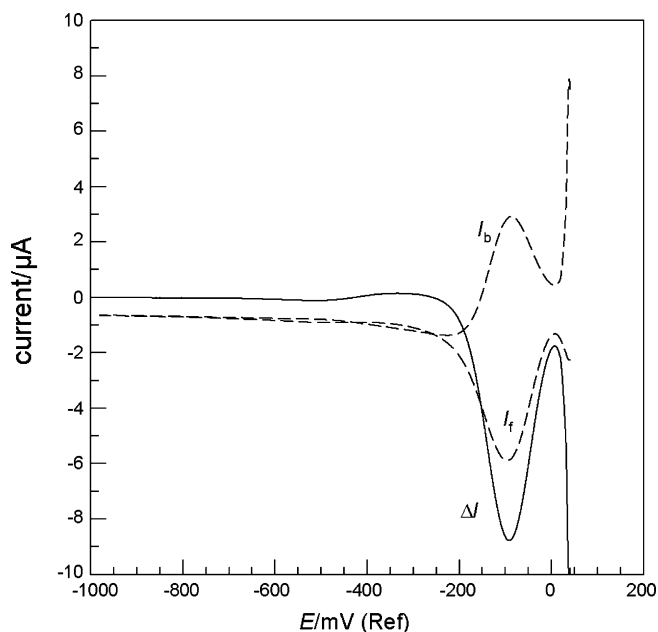


Fig. 1. Individual forward  $I_f$  and backward  $I_b$  currents and differential current  $\Delta I = I_f - I_b$  in SWV performed at SMDE with a reductive direction using a solution of  $5.6 \times 10^{-3} \text{ mol dm}^{-3}$  Ce(IV) in  $1.42 \text{ mol dm}^{-3}$   $\text{Na}_2\text{CO}_3/0.13 \text{ mol dm}^{-3}$   $\text{NaHCO}_3$  at  $25^\circ\text{C}$ . The other experimental conditions are:  $\Delta t = 20 \text{ ms}$ ,  $\Delta E_s = -4 \text{ mV}$  and  $E_{sw} = -80 \text{ mV}$ .

of Ce(IV) at the electrode surface is equal to  $c^*$ ,  $c^*$  being the initial Ce(IV) bulk concentration. An oxidative direction was performed in the positive direction, starting at a potential where the concentration of Ce(IV) at the electrode surface tends to zero, i.e. the concentration of Ce(III) is equal to  $c^*$  [24].

The apparent diffusion coefficient of Ce(IV),  $D_{IV}$ , was calculated from the limiting current,  $I_L$  [25] measured by direct current polarography, assuming a reversible behaviour for the Ce(IV)/Ce(III) couple:

$$|I_L| = \frac{FA\sqrt{D_{IV}c^*}}{\sqrt{\pi T_G}} \left( 1 + \frac{\sqrt{\pi D_{IV} T_G}}{r_0} \right) \quad (2)$$

$A$  and  $r_0$  are the area and the radius of the static mercury drop electrode, respectively and  $T_G$  is the drop time. Subscripts IV and III are used in this work for parameters related to Ce(IV) and Ce(III), respectively.  $D_{IV}$  was also determined from the CV peak current [26]

$$|I_p| = 0.4463 FAc^* \left( \frac{F}{RT} \right)^{1/2} v^{1/2} D_{IV}^{1/2} \quad (3)$$

where  $v$  is the scan rate and from the SWV differential peak current [21,22]

$$|\Delta I_p| = \frac{1.2\varphi FAc^*\sqrt{D_{IV}}}{\sqrt{\pi\Delta t}} \quad (4)$$

where  $\varphi = (\sqrt{\xi} - 1)/(\sqrt{\xi} + 1)$ . The SWV measurements show also that

$$E_p^o = E_p^r = E_{1/2}(T) \quad (5)$$

with  $E_p^o$  and  $E_p^r$  are the peak potentials obtained during the reductive and oxidative directions, respectively.

#### 3.2. Ionic strength corrections

$$p = \frac{m}{c} \quad (6)$$

is the molar–molal conversion factor between molal ( $\text{mol kg}^{-1}$ ) and molar ( $\text{mol dm}^{-3}$ ) concentrations. For each salt, the  $p$  values are given in [5]. We define

$$q = \log_{10} \frac{p}{m} \quad (7)$$

From molar equilibrium constant  $K = \prod_i c_i^{v_i}$ , molal equilibrium constant

$$K_m = \prod_i m_i^{v_i} = p^{\Delta_r v} K \quad (8)$$

is calculated, where  $v_i$  is a stoichiometric coefficient (it is positive for products, negative for reactants) and  $\Delta_r v = \sum_i v_i$ . When the electrolyte is a mixture of three salts ( $\text{Na}_2\text{CO}_3$ ,  $\text{NaHCO}_3$ ,  $\text{NaNO}_3$ )  $q$  is assumed to be constant for each salt, and the approximation

$$\log_{10} p \approx q_{\text{Na}_2\text{CO}_3} m_{\text{Na}_2\text{CO}_3} + q_{\text{NaHCO}_3} m_{\text{NaHCO}_3} + q_{\text{NaNO}_3} m_{\text{NaNO}_3} \quad (9)$$

Table 1  
Physical parameters  $q_X$  and  $r_X$  relative to the pure salt X used in this study

Electrolyte X	$q_X$	$r_X$
Na <sub>2</sub> CO <sub>3</sub>	0.00574	-0.01632
NaHCO <sub>3</sub>	0.01276	-0.01359
NaNO <sub>3</sub>	0.01453	-0.01453

was used. We used similar notation and approximation for calculating  $a_{H_2O}$ , the activity of water:

$$\log_{10} a_{H_2O} = \sum r m \quad (10)$$

where  $r$  is an empirical value for each salt, and in our mixtures

$$\log_{10} a_{H_2O} \approx r_{Na_2CO_3} m_{Na_2CO_3} + r_{NaHCO_3} m_{NaHCO_3} + r_{NaNO_3} m_{NaNO_3} \quad (11)$$

Numerical values of  $q$  and  $r$  are given in Table 1.

The basic specific ion interaction theory (SIT) [27,28,5] model, based on the Brönsted-Guggenheim-Scatchard principle [29–34] was already applied to the cerium in carbonate solutions [10,35]. It can be expressed by the equation for activity coefficients for high ionic strengths [36,37]

$$\log_{10} \gamma_i = -z_i^2 H_{I_m, T} + \sum_j (\varepsilon(i, j) m_j) \quad (12)$$

with  $\gamma_i$  and  $z_i$  are the activity coefficient and the charge of ion  $i$ , respectively and where

$$H_{I_m, T} = \frac{A_m(T) \sqrt{I_m}}{1 + b_m(T) \sqrt{I_m}} \quad (13)$$

is Debye–Hückel equation.  $D_{I_m, T}$  is the usual notation for  $H_{I_m, T}$ , but here we have already used  $D$  notation for the diffusion coefficient.  $A_m(T)$  and  $b_m(T)$  are physical parameters, their values are given in Table 2 in the temperature range under study— $\varepsilon(i, j)$  is the specific interaction coefficient for short range specific interactions between ions  $i$  and  $j$  with charges of opposite signs and is assumed to be equal to zero for neutral species and for ions having same sign.  $m_j$  is the molal concentration of species  $j$  and  $I_m$  is the molal ionic strength. Typically, for our reference

Table 2  
Physical parameters used for Debye–Hückel equation

$T/^\circ\text{C}$	$A_m(T)/\text{kg}^{1/2} \text{mol}^{-1/2}$	$b_m(T)/\text{kg}^{1/2} \text{mol}^{-1/2}$
5	0.494	1.486
10	0.498	1.489
15	0.501	1.493
20	0.505	1.497
25	0.509	1.500
30	0.513	1.504
35	0.518	1.507
40	0.525	1.513
45	0.529	1.516
50	0.534	1.519

Table 3  
The specific interaction coefficients  $\varepsilon(i, j)$  ( $\text{kg mol}^{-1}$ ) determined by the SIT model [5]

$\varepsilon(i, j)$	$j = \text{CO}_3^{2-}$	$j = \text{HCO}_3^-$	$j = \text{NO}_3^-$	$j = \text{OH}^-$
$i = \text{Na}^+$	$-0.08 \pm 0.03$	$0.00 \pm 0.02$	$0.00 \pm 0.02$	$0.04 \pm 0.01$
$i = \text{H}^+$	$0.00 \pm 0.05$	$0.07 \pm 0.05$	$0.07 \pm 0.05$	$0.00 \pm 0.01$

electrode, we used

$$\log_{10} \gamma_{\text{Cl}^-, \text{Ref}} = -H_{I_m, T} + \varepsilon(\text{Cl}^-, \text{Na}^+) m_{\text{Na}^+} \quad (14)$$

where [38,39]

$$\varepsilon(\text{Cl}^-, \text{Na}^+) = 0.034 + 3.7 \times 10^4 \Delta T - 6.2 \times 10^6 \Delta T^2 \quad (15)$$

with  $\Delta T = T - T^0$  and  $T^0 = 298.15 \text{ K}$ .

Activity corrections for equilibrium constants,  $K_m$ , is calculated as:

$$\log_{10} K_m(0) = \log_{10} K_m - \Delta_r z^2 H_{I_m, T} + \sum_j \Delta_r \varepsilon(j) m_j + \nu_{H_2O} \log_{10} a_{H_2O} \quad (16)$$

where  $K_m(0)$  is the equilibrium constant at zero ionic strength,  $\Delta_r z^2 = \sum_i \nu_i z_i^2$  and  $\Delta_r \varepsilon(j) = \sum_i \nu_i \varepsilon(i, j)$ . Typically for constant  $K_{lm} = m_{\text{HCO}_3^-} / (m_{\text{CO}_3^{2-}} m_{\text{H}^+})$  in our mixtures, taking into account  $\nu_{H_2O} = 0$ , Eq. (16) is written

$$\log_{10} K_{lm} = \log_{10} K_{lm}(0) + \Delta_r z^2 H_{I_m, T} - \Delta_r \varepsilon(\text{Na}^+) m_{\text{Na}^+} - \Delta_r \varepsilon(\text{NO}_3^-) m_{\text{NO}_3^-} - \Delta_r \varepsilon(\text{CO}_3^{2-}) m_{\text{CO}_3^{2-}} - \Delta_r \varepsilon(\text{HCO}_3^-) m_{\text{HCO}_3^-} \quad (17)$$

where  $\log_{10} K_{lm}(0) = 10.329 \pm 0.020$  at  $25^\circ\text{C}$  [3],  $\Delta_r z^2 = -4$  and with

$$\Delta_r \varepsilon(\text{Na}^+) = \varepsilon(\text{HCO}_3^-, \text{Na}^+) - \varepsilon(\text{CO}_3^{2-}, \text{Na}^+) - \varepsilon(\text{NO}_3^-, \text{Na}^+) \quad (18)$$

$$\Delta_r \varepsilon(\text{NO}_3^-) = -\varepsilon(\text{H}^+, \text{NO}_3^-) \quad (19)$$

$$\Delta_r \varepsilon(\text{HCO}_3^-) = -\varepsilon(\text{H}^+, \text{HCO}_3^-) \quad (20)$$

$$\Delta_r \varepsilon(\text{CO}_3^{2-}) = -\varepsilon(\text{H}^+, \text{CO}_3^{2-}) \quad (21)$$

The  $\varepsilon(i, j)$  values are given in Table 3.

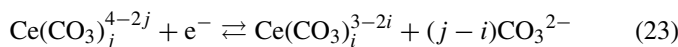
Similarly,  $K_{2m} = m_{\text{CO}_2} / (m_{\text{HCO}_3^-} m_{\text{H}^+})$  was calculated from  $\log_{10} K_{2m}(0) = 6.354 \pm 0.020$  at  $25^\circ\text{C}$  [3] and using Eq. (16).  $K_{1m}$ ,  $K_{2m}$ , ionic product of water  $K_{em}$  (where  $\log_{10} K_{em}(0) = m_{\text{OH}^-} a_{\text{H}^+} = -14.001 \pm 0.0140$  at  $25^\circ\text{C}$  [1]) values and the following mass balance equation

$$m_{\text{Na}^+} + m_{\text{H}^+} = 2m_{\text{CO}_3^{2-}} + m_{\text{HCO}_3^-} + m_{\text{OH}^-} + m_{\text{NO}_3^-} \quad (22)$$

were used for calculating,  $m_{\text{Na}^+}$ ,  $m_{\text{CO}_3^{2-}}$ ,  $m_{\text{HCO}_3^-}$ ,  $m_{\text{H}^+}$  and  $m_{\text{OH}^-}$ . This speciation was calculated at  $25^\circ\text{C}$  in a given solution. Since  $m_{\text{CO}_3^{2-}}$  did not change with the temperature, this is enough for interpreting the influence  $m_{\text{CO}_3^{2-}}$  on our redox measurements in the  $5\text{--}50^\circ\text{C}$  temperature range.

### 3.3. Redox potential of the Ce(IV)/Ce(III) couple and temperature influence on this potential

The test solutions used in this work are pH buffered solutions, thus it is not possible to detect possible differences in the hydroxide speciations with Ce(IV) and Ce(III), only the Ce-carbonate speciations were studied. Then, the redox reaction can be written



and the Nernst law corresponding to this reaction is

$$E(T) = E_{\text{IVj/IIIi}}^0(T) + r_f T \log_{10} \frac{m_{\text{Ce}(\text{CO}_3)_j^{4-2j}}}{m_{\text{Ce}(\text{CO}_3)_i^{3-2i}}} - r_f T (j-i) \log_{10} m_{\text{CO}_3^{2-}} \quad (24)$$

( $j-i$ ), the stoichiometric coefficient difference and

$$E_{\text{IVj/IIIi}}^0(T) = E_{\text{IVj/IIIi}}^0(T) + r_f T \log_{10} \frac{\gamma_{\text{Ce}(\text{CO}_3)_j^{4-2j}}}{\gamma_{\text{Ce}(\text{CO}_3)_i^{3-2i}} \gamma_{\text{CO}_3^{2-}}^{j-i}} \quad (25)$$

is the normal potential of  $\text{Ce}(\text{CO}_3)_j^{4-2j}/\text{Ce}(\text{CO}_3)_i^{3-2i}$  redox system.

For temperature influence, we used the following equations and approximations [38]

$$\Delta_r G_T = -RT \ln K = -FE_{1/2}(T) \quad (26)$$

$$\Delta_r G_T \approx \Delta_r G_{T^0} - \Delta_r S_{T^0} \Delta T \quad (27)$$

According to Eqs. (26) and (27), the half-wave potential writes

$$E_{1/2}(T) \approx E_{1/2}(T^0) + \frac{\Delta_r S_{T^0}}{F} \Delta T \quad (28)$$

A linear relation exists between  $E_{1/2}(T)$  and  $\Delta T$ ;  $\Delta_r S_{T^0}$  was calculated from the corresponding slope.

This first order approximation is also equivalent to

$$\frac{E_{1/2}(T)T^0}{T} \approx -\frac{\Delta_r G_{T^0}}{F} - \frac{\Delta_r H_{T^0}T^0}{F} \Delta \left( \frac{1}{T} \right) \quad (29)$$

a classical Van't Hoff plot, where  $\Delta(1/T) = 1/T - 1/T^0$ . We also used the slope of such linear plot for a direct determination of  $\Delta_r H_{T^0}$ .

## 4. Results and discussion

### 4.1. Reversibility of the Ce(IV)/Ce(III) redox couple and determination of apparent diffusion coefficient $D_{\text{IV}}$

The potential of the Ce(IV)/Ce(III) redox couple was measured in carbonate/bicarbonate solutions using three electrochemical techniques: direct current polarography, cyclic voltammetry and square wave voltammetry. An illustration of experimental curves is given in Fig. 2 for  $5.3 \times 10^{-3} \text{ mol dm}^{-3}$  Ce(IV) in  $1.42 \text{ mol dm}^{-3} \text{ Na}_2\text{CO}_3/0.13 \text{ mol dm}^{-3} \text{ NaHCO}_3$ .

Whatever the carbonate/bicarbonate solution used in this study, data resulting from electrochemical techniques clearly

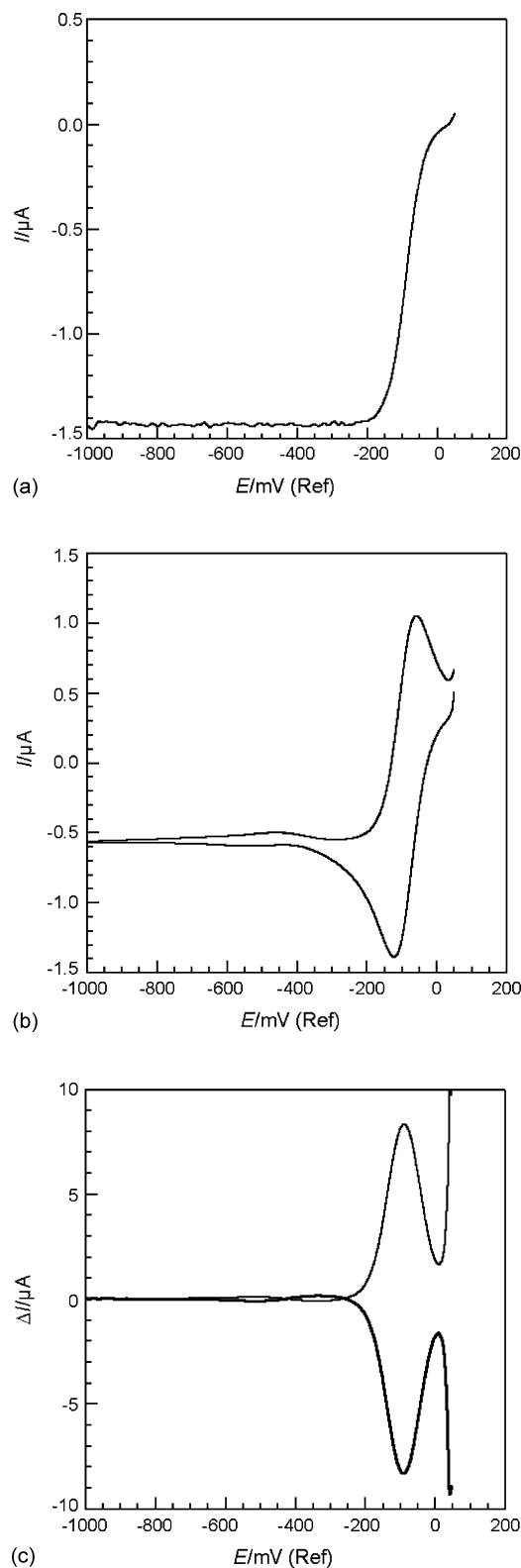


Fig. 2. Curves of  $5.3 \times 10^{-3} \text{ mol dm}^{-3}$  Ce(IV) in  $1.42 \text{ mol dm}^{-3} \text{ Na}_2\text{CO}_3/0.13 \text{ mol dm}^{-3} \text{ NaHCO}_3$  at  $25^\circ\text{C}$  obtained by DCP (a), CV (b) and SWV obtained with reductive and oxidative directions (c). The experimental conditions are: for DCP  $T_G = 1 \text{ s}$ , for CV  $v = 50 \text{ mV s}^{-1}$  and for SWV  $\Delta t = 20 \text{ ms}$ ,  $|\Delta E_s| = 4 \text{ mV}$ ,  $|E_{\text{sw}}| = 80 \text{ mV}$  and for the oxidative direction the initial potential is  $E_1 = -1 \text{ V/Ref}$ .

evidence that the Ce(IV)/Ce(III) couple is reversible. The reversibility was first evidenced from DCP results. In the case of a reversible system, the potential varies linearly with  $\log_{10}((I_L - I)/I)$ ;  $I_L$  is the limiting current and the corresponding slope is  $r_f T$ . Our experimental DPC results give linear relationships with slope values of  $59.0 \pm 2.5$  mV and  $66.0 \pm 2.5$  mV at 25 °C and 50 °C, respectively; these values are close to the theoretical ones, 59.2 mV at 25 °C and 64.1 mV at 50 °C. CV results are consistent with this result because the anodic and the cathodic peak potentials were found to be separated by  $60.0 \pm 2.5$  mV at 25 °C and  $66.0 \pm 2.5$  mV at 50 °C, when  $0.05 \leq v/V \text{ s}^{-1} \leq 0.5$ ; the theoretical difference between the anodic and cathodic peaks for a reversible and monoelectronic system is equal to 56.5 mV at 25 °C and 61.3 mV at 50 °C [26]. For the CV measurements, we also checked the linearity between the anodic and cathodic peak currents and the square root of  $v$ . The reversibility of the Ce(IV)/Ce(III) couple in our carbonate/bicarbonate mixtures, was finally confirmed by SWV results for  $10 \leq \Delta t/\text{ms} \leq 62.5$ . Indeed, for  $|E_{\text{sw}}| = 80$  mV, the half-height widths of SWV waves at 25 °C were close to  $112.0 \pm 2.5$  mV, a value consistent with the theoretical one, 113.0 mV [22,40]. Finally, the two symmetrical waves with respect to the potential axis in the 15–50 °C range are also a characteristic feature of a reversible system [23].

The limiting current,  $I_L$ , obtained by DCP and the peak currents,  $I_p$  and  $\Delta I_p$ , obtained by CV and SWV, vary linearly as a function of Ce(IV) concentration ( $c^*$ ) between  $10^{-2}$  mol dm $^{-3}$  and  $10^{-3}$  mol dm $^{-3}$ .  $\text{CO}_3^{2-}$  concentration has no influence on these three currents. At a temperature and an ionic strength, an average Ce(IV) apparent diffusion coefficient,  $D_{\text{IV}}$ , in carbonate/bicarbonate media, was computed from the three values obtained by DCP (Eq. (2)), CV (Eq. (3)) and SWV (Eq. (4)); and for two compositions of test solutions ( $1.42$  mol dm $^{-3}$   $\text{Na}_2\text{CO}_3/0.13$  mol dm $^{-3}$   $\text{NaHCO}_3$ ;  $I_c = 4.39$  mol dm $^{-3}$  and  $1.03$  mol dm $^{-3}$   $\text{Na}_2\text{CO}_3/0.20$  mol dm $^{-3}$   $\text{NaHCO}_3$ ;  $I_c = 3.29$  mol dm $^{-3}$ ). Ce(IV) concentration was  $5.3 \times 10^{-4}$  mol dm $^{-3}$ , the pH of these two solutions is  $10.5 \pm 0.2$  at 25 °C and the uncertainty on  $D_{\text{IV}}$  is less than 10%.  $D_{\text{IV}}$  values (Table 4) increase when the ionic strength decreases or when the temperature increases. This last feature suggests that the Ce behaviour is same for  $I_c = 4.39$  mol dm $^{-3}$  and  $3.29$  mol dm $^{-3}$  and that the  $D_{\text{IV}}$  increasing with the ionic strength decreasing is probably due to the viscosity difference between the two test solutions.

Table 4  
Apparent diffusion coefficient of Ce(IV),  $D_{\text{IV}}$ , deduced from Eqs. (2)–(4)

$T/^\circ\text{C}$	$I_c = 4.39$ mol dm $^{-3}$	$I_c = 3.29$ mol dm $^{-3}$
5	0.52	0.65
15	0.80	1.04
20	1.03	1.21
25	1.14	1.45
35	1.72	2.05
50	2.89	3.30

<sup>a</sup> Average of three  $D_{\text{IV}}$  values obtained by DCP, CV and SWV.

#### 4.2. Stoichiometry of limiting complexes

The stoichiometry of predominant Ce(IV) and Ce(III) complexes in carbonate/bicarbonate media in the temperature range 5–50 °C was investigated as follows.  $E_{1/2}(T)$  values were determined from SWV curves in  $\text{Na}_2\text{CO}_3/\text{NaHCO}_3/\text{NaNO}_3$  solutions with different compositions and plotted as a function of  $\text{CO}_3^{2-}$  molal concentration,  $m_{\text{CO}_3^{2-}}$ . The ionic strength was maintained constant at  $4.39$  mol dm $^{-3}$  in all the experiments by adding  $\text{NaNO}_3$ . The initial molar concentrations  $[\text{Na}_2\text{CO}_3]$ ,  $[\text{NaHCO}_3]$ ,  $[\text{NaNO}_3]$  and  $I_m$ ,  $m_{\text{Na}^+}$ ,  $m_{\text{CO}_3^{2-}}$ ,  $m_{\text{HCO}_3^-}$ ,  $-\log_{10} m_{\text{OH}^-}$  and  $-\log_{10} m_{\text{H}^+}$  values calculated from the initial conditions and Eqs. (6–22) are listed in Table 5. The  $E_{1/2}(T)$  values obtained in different solutions and temperatures are listed in Table 6. First, we examine results obtained at 25 °C. A linear  $E_{1/2}(T) - \log_{10} m_{\text{CO}_3^{2-}}$  relationship was found (Fig. 3); the corresponding slope is equal to  $-107.6$  mV. A value equal to 1.82 is obtained after dividing by  $r_f T$ . Refinements of experimental data using Eq. (23) were done, assuming the exchange of either one  $\text{CO}_3^{2-}$  ion (dotted line with a slope of  $-59.2$  mV and  $E_{\text{IV/III}}^0(T) = 232.0 \pm 2.5$  mV/S.H.E.) or two  $\text{CO}_3^{2-}$  ions (dashed line with a slope of  $-118.4$  mV and  $E_{\text{IV/III}}^0(T) = 237.0 \pm 2.5$  mV/S.H.E.) with respect to one electron during the redox reaction and no complex dissociation are reported in Fig. 3. Examination of this figure supports a value of 2 for  $(j - i)$ . As it will be shown later,  $(j - i)$  is close to 2 and the difference is due to a dissociation of the limiting carbonate complexes.

Starting from the well-established stoichiometry of Ce(III) limiting complex,  $\text{Ce}(\text{CO}_3)_4^{5-}$  [11], the exchange of two  $\text{CO}_3^{2-}$  ions enables us to suggest the following stoichiometry for the Ce(IV) limiting complex,  $\text{Ce}(\text{CO}_3)_6^{8-}$ . This result deduced

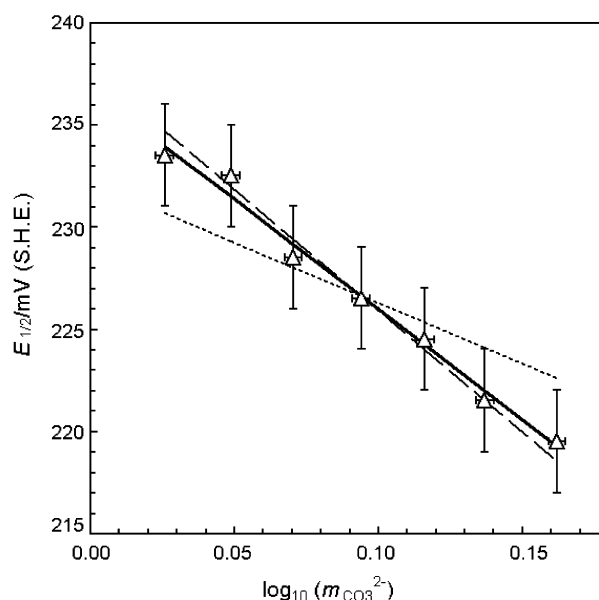


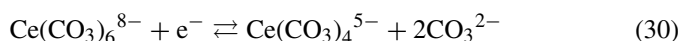
Fig. 3. Influence of the  $\text{CO}_3^{2-}$  molal concentration on the half-wave potential of the  $\text{Ce}(\text{CO}_3)_6^{8-}/\text{Ce}(\text{CO}_3)_4^{5-}$  redox couple measured by SWV in carbonate/bicarbonate media at 25 °C. Solid lines are fitted using Eq. (33). The dotted and dashed lines were plotted from Eq. (23) assuming the exchange of either one or two  $\text{CO}_3^{2-}$  ions per electron during the redox reaction.

Table 5

Compositions and molal ionic strengths ( $I_m$ ) of test solutions and molal concentrations ( $m$ ) of ions in solution

No.	Initial solutions (mol dm <sup>-3</sup> )			Values calculated (mol kg <sup>-1</sup> )					
	[Na <sub>2</sub> CO <sub>3</sub> ]	[NaHCO <sub>3</sub> ]	[NaNO <sub>3</sub> ]	$I_m$	$m_{Na^+}$	$m_{CO_3^{2-}}$	$m_{HCO_3^-}$	$-\log_{10} m_{OH^-}$	$-\log_{10} m_{H^+}$
1	1.00	0.10	1.29	4.67	3.60	1.06	0.11	3.64	10.11
2	1.06	0.11	1.10	4.63	3.52	1.12	0.12	3.64	10.08
3	1.12	0.12	0.92	4.62	3.45	1.18	0.13	3.65	10.06
4	1.19	0.12	0.70	4.58	3.34	1.24	0.13	3.61	10.08
5	1.26	0.13	0.48	4.55	3.25	1.31	0.14	3.61	10.06
6	1.33	0.13	0.27	4.53	3.16	1.37	0.13	3.57	10.08
7	1.42	0.13	0	4.49	3.04	1.45	0.13	3.53	10.10

from SWV curves corroborates the conclusions of previous electrochemical studies based on emf measurements [35] or CV curves [10]. This formula is consistent with the coordination chemistry of Ce(IV) proposed in [41,42]. Note that our methodology did not allow the determination of Na<sup>+</sup> ions in the limiting complex that may partially neutralize the large negative charge as it was done in [35]. The stoichiometry of Ce(IV) and Th(IV) [12,13] limiting complexes is identical but it differs from the stoichiometry, An(CO<sub>3</sub>)<sub>5</sub><sup>6-</sup>, commonly-proposed for some actinides(IV): U [2,43], Pu [38], Np [44] at similar ionic strengths. The difference in stoichiometry is probably due to the larger ionic radius size of cerium and thorium. Assuming Ce(CO<sub>3</sub>)<sub>6</sub><sup>8-</sup> and Ce(CO<sub>3</sub>)<sub>4</sub><sup>5-</sup> are predominant species in solutions, the following redox reaction can be proposed



and the Nernst law writes

$$E(T) = E_{IV_6/III_4}^0(T) + r_f T \log_{10} \frac{m_{Ce(CO_3)_6^{8-}}}{m_{Ce(CO_3)_4^{5-}}} - 2r_f T \log_{10} m_{CO_3^{2-}} \quad (31)$$

For simplicity we now use notations  $E_{IV/III}^0(T)$  and  $E_{IV/III}^0(T)$  for  $E_{IV_6/III_4}^0(T)$  and  $E_{IV_6/III_4}^0(T)$ , respectively. As experimental ( $j-i$ ) value is slightly lower than 2, we should consider a par-

tial dissociation of the Ce(IV) and Ce(III) limiting complexes into Ce(CO<sub>3</sub>)<sub>5</sub><sup>6-</sup> [12,13,45] and Ce(CO<sub>3</sub>)<sub>3</sub><sup>3-</sup> [11], respectively. Consequently, a refinement of the treatment of the experimental data was done substituting the following equation

$$E_{1/2}(T) = E_{IV_j/III_i}^0(T) + r_f T \log_{10} \left( \frac{D_{III}}{D_{IV}} \right)^{1/2} \quad (32)$$

into Eq. (31) which becomes

$$E_{1/2}(T) = E_{IV/III}^0(T) + r_f T \left( \log_{10} \frac{\alpha_{III}}{\alpha_{IV}} - 2 \log_{10} m_{CO_3^{2-}} \right) \quad (33)$$

Indeed, at  $E_{1/2}(T)$ , Ce(IV) concentration is equal to Ce(III) concentration at the electrode surface.  $\alpha_{III} = 1 + 1/K_{III,4} m_{CO_3^{2-}}$  and  $\alpha_{IV} = 1 + 1/K_{IV,6} m_{CO_3^{2-}}$  are the Ringbom coefficients,  $K_{IV,6} = m_{Ce(CO_3)_6^{8-}} / m_{Ce(CO_3)_5^{6-}} m_{CO_3^{2-}}$  and  $K_{III,4} = m_{Ce(CO_3)_4^{5-}} / m_{Ce(CO_3)_3^{3-}} m_{CO_3^{2-}}$ .

In Eq. (33), the ratio  $r_f T \log_{10} (D_{III}/D_{IV})^{1/2} \approx 0$ . Indeed, our experimental results have shown that  $D_{III} \approx D_{IV}$  ( $D_{IV}$  values are given in Table 4) whatever the temperature because the SWV differential peak currents,  $|\Delta I_p^{\text{reductive}}|$  and  $|\Delta I_p^{\text{oxidative}}|$ , obtained with reductive and oxidative directions, respectively, are identical, according to Eq. (4),  $|\Delta I_p^{\text{reductive}}| = \Psi \sqrt{D_{IV}}$  and  $|\Delta I_p^{\text{oxidative}}| = \Psi \sqrt{D_{III}}$  where  $\Psi = 1.2 \varphi F A c^* / \sqrt{\pi \Delta t}$ .

Table 6

Influence of the CO<sub>3</sub><sup>2-</sup> molal concentration on the measured potential,  $E_{1/2}(T)$ 

No.	$E_{1/2}(T)/mV$ (S.H.E.)					
	$T=5^\circ C$	$T=10^\circ C$	$T=15^\circ C$	$T=25^\circ C$	$T=45^\circ C$	$T=50^\circ C$
1	263.0	257.5	252.0	233.5	206.0	191.0
2	259.0			232.5		190.0
3	255.0	252.0	247.5	228.5	201.5	187.0
4	252.0			226.5		183.0
5	249.0	244.0	241.5	224.5	195.0	182.0
6	245.0			221.5		177.0
7	242.0	237.0	238.0	219.5	190.0	175.0
$E_{IV/III}^0(T)$			259.5	243.0	215.5	198.0
$\log_{10} K_{IV,6}$			0.42	0.50	0.56	0.97
$\log_{10} K_{III,4}$			0.88	1.50 <sup>a</sup>	5.03	7.00
$a/(r_f T)^b$	-2.78	-2.69	-1.86	-1.82	-1.82	-1.93

The compositions of test solutions are those of Table 5. The experimental  $E_{1/2}(T)$  data (upper part of the table) were fitted from Eq. (33).  $E_{IV/III}^0(T)$ ,  $K_{IV,6}$  and  $K_{III,4}$  (lower part of the table) were fitted from the  $E_{1/2}(T)$  data in the same column.

<sup>a</sup>  $\log_{10} K_{III,4}$  value given by Ferri et al. [11].

<sup>b</sup>  $a$  is the slope of the linear regression of experimental data.

During the refinement procedure, at 25 °C,  $\log_{10} K_{\text{III},4}$  was maintained at 1.50 [11], while  $\log_{10} K_{\text{IV},6}$  and  $E_{\text{IV/III}}^0(T)$  were numerically fitted. The best correlation between theoretical and experimental data was found with  $\log_{10} K_{\text{IV},6} = 0.50$  and  $E_{\text{IV/III}}^0(T) = 243.0 \pm 2.5 \text{ mV/S.H.E.}$  The huge shift of the normal potential in carbonate solutions from the data value (230.7 mV/S.H.E.) was already reported in [35] and was attributed to a difference in the stability of the two limiting complexes. The Ringbom coefficients were then calculated from  $K_{\text{III},4}$  and  $K_{\text{IV},6}$  values. Fig. 4 reports the  $\text{Ce}(\text{CO}_3)_6^{8-}$  and  $\text{Ce}(\text{CO}_3)_4^{5-}$  as a function of  $\text{CO}_3^{2-}$  molal concentration; it points out a dissociation of  $\text{Ce}(\text{CO}_3)_6^{8-}$  into  $\text{Ce}(\text{CO}_3)_5^{6-}$  and a negligible dissociation of  $\text{Ce}(\text{CO}_3)_4^{5-}$  into  $\text{Ce}(\text{CO}_3)_3^{3-}$ .  $K_{\text{IV},6}$  value obtained here is close to that proposed in [10] in which the  $\text{Ce}(\text{CO}_3)_6^{8-}$  dissociation was indicated as a possible objective for further studies in conclusion.

$E_{1/2}(T) - \log_{10} m_{\text{CO}_3^{2-}}$  plots at 15, 25, 45 and 50 °C are presented in Fig. 5. The experimental data were fitted from Eq. (33):  $\log_{10} K_{\text{III},4}$ ,  $\log_{10} K_{\text{IV},6}$  and  $E_{\text{IV/III}}^0(T)$  were adjusted by successive iterations in order to obtain a good fitting between theoretical and experimental data. Corresponding values are given in Table 6. The ratios ( $a/r_f T$ ) where  $a$  is the slope of linear regressions of  $E_{1/2}(T) = f(\log_{10} m_{\text{CO}_3^{2-}})$  are also listed in this table. In the temperature range 15–50 °C, the ratio value is close to  $-2$  suggesting that the predominant system is always:  $\text{Ce}(\text{CO}_3)_6^{8-}/\text{Ce}(\text{CO}_3)_4^{5-}$ . But, the ratio decreases at temperatures lower than 15 °C. Therefore, the procedure used for the temperatures upper to 15 °C is not valid. This difference at low temperature is also evidenced with examination of SWV results. Indeed, the waves obtained by SWV during the forward and reverse scans are not symmetrical with respect of the potential axis; the difference between the two peak potentials is higher than 6 mV. Modifications of the Ce(IV)/Ce(III)

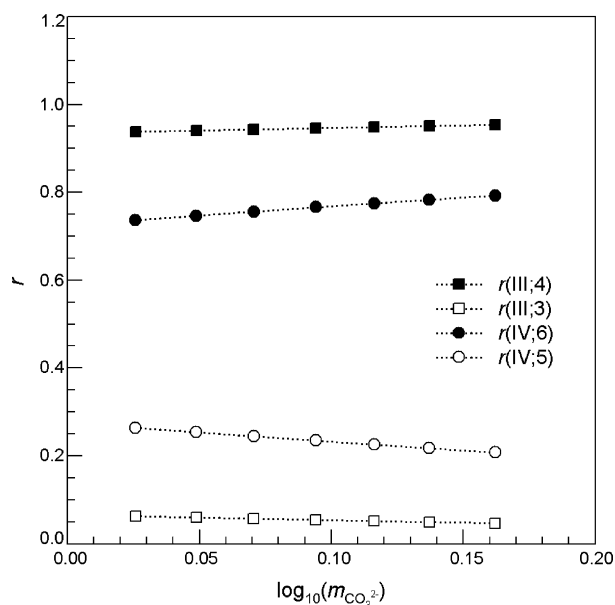


Fig. 4. Influence of the  $\text{CO}_3^{2-}$  molal concentration on the molar fractions of Ce(IV) and Ce(III) complexes:  $r(\text{III}; 4) = [\text{Ce}(\text{CO}_3)_4^{5-}]/c^*$ ,  $r(\text{III}; 3) = [\text{Ce}(\text{CO}_3)_3^{3-}]/c^*$ ,  $r(\text{IV}; 6) = [\text{Ce}(\text{CO}_3)_6^{8-}]/c^*$  and  $r(\text{IV}; 5) = [\text{Ce}(\text{CO}_3)_5^{6-}]/c^*$ .

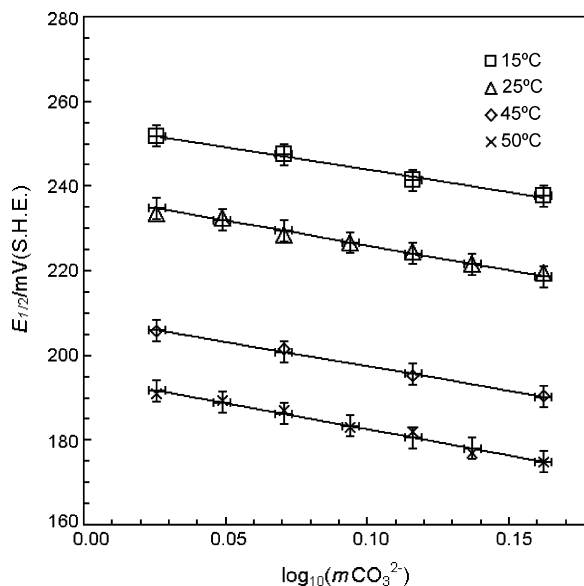


Fig. 5. Influence of the  $\text{CO}_3^{2-}$  molal concentration on the  $E_{1/2}(T)$  potential measured by SWV at four temperatures. Solid lines result from the fitting of experimental data using Eq. (33).

system behaviour below 15 °C could be attributed either to a precipitation of the limiting complexes or to an increasing concentration of other complexes than  $\text{Ce}(\text{CO}_3)_6^{8-}$  and  $\text{Ce}(\text{CO}_3)_4^{5-}$ .

#### 4.3. Estimation of entropy and enthalpy

The  $E_{1/2}(T) - T$  and  $E_{\text{IV/III}}^0(T) - T$  linear relationships allowed us to estimate the reaction entropy  $\Delta_r S_{T^0}$  and enthalpy  $\Delta_r H_{T^0}$ , from Eqs. (26)–(29) (see Section 3.3). Only data in the 15–50 °C temperature range were used. The  $E_{1/2}(T)$  values determined from SWV experiments were plotted as a function of  $T$  at two ionic strengths,  $I_c = 4.39 \text{ mol dm}^{-3}$  and  $I_c = 3.29 \text{ mol dm}^{-3}$  corresponding to the following solutions:  $1.42 \text{ mol dm}^{-3} \text{ Na}_2\text{CO}_3/0.13 \text{ mol dm}^{-3} \text{ NaHCO}_3$  and  $1.03 \text{ mol dm}^{-3} \text{ Na}_2\text{CO}_3/0.20 \text{ mol dm}^{-3} \text{ NaHCO}_3$ . The  $E_{1/2}(T)$  values reported in Table 7 were expressed in V/S.H.E. by subtracting  $E_{\text{Ref}}(T)$  from experimental data. The  $E_{\text{IV/III}}^0(T)$  fitted values (see Section 4.2) are also recalled in this table. The  $E_{1/2}(T)$  and  $E_{\text{IV/III}}^0(T)$  values are plotted as a function of  $T$  in Fig. 6. Examination of this figure shows that both an increase of the ionic strength at a given temperature and an increase of the temperature in the 15–50 °C range at a given ionic strength, lead to a decrease of  $E_{1/2}(T)$ . Linear regressions of experimental data (dashed and solid lines in Fig. 6) allow a right estimation of  $\Delta_r S_{T^0}$ , according to Eq. (28) which becomes

$$E_{1/2}(T) \approx \left( E_{1/2}(T^0) - \frac{\Delta_r S_{T^0}}{F} T^0 \right) + \frac{\Delta_r S_{T^0}}{F} T \quad (34)$$

The  $E_{1/2}(T)T^0/T$  and  $E_{\text{IV/III}}^0(T)T^0/T$  variations with  $T^0/T$  are presented in Fig. 7. A numerical value of  $\Delta_r H_{T^0}$  was determined from the slope of linear regressions (dashed and solid

Table 7  
Temperature influence on the  $E_{1/2}(T)$ ,  $E_{IV/III}^{0'}(T)$  and  $E_{Ref}(T)$  potentials (upper part of the table)

$T/^\circ\text{C}$	$E_{Ref}(T)^a/\text{mV}$ (S.H.E.)		$E_{1/2}(T)/\text{mV}$ (S.H.E.)		$E_{IV/III}^{0'}(T)^b/\text{mV}$ (S.H.E.)
	$I_c = 3.29 \text{ mol dm}^{-3}$	$I_c = 4.39 \text{ mol dm}^{-3}$	$I_c = 3.29 \text{ mol dm}^{-3}$	$I_c = 4.39 \text{ mol dm}^{-3}$	$I_c = 4.39 \text{ mol dm}^{-3}$
15	331.0	331.5	237.0	230.5	259.5
20	329.0	330.0	232.5	219.0	
25	327.0	327.5	222.5	214.5	243.0
30	325.0	325.0		208.0	
35	322.5	323.0	209.5	201.0	
45	318.5	318.5			215.5
50	315.0	316.0	189.0	180.0	198.0
		$FT^0\text{slope}^c/\text{kJ mol}^{-1}$	Calculated from the experimental data		Calculated from fitted values
			−38	−39	$-46 \approx T^0 \Delta_r S_{T^0}$
		$F\text{slope}^d/\text{kJ mol}^{-1}$	−59	−59	$-70 \approx \Delta_r H_{T^0}$

The values of the entropy  $\Delta_r S_{T^0}$  and the enthalpy  $\Delta_r H_{T^0}$  (lower part of the table) deduced from the  $E(T)$  values in the same column by using Eqs. (34) and (35).

<sup>a</sup> Calculated from the following equation:  $E_{Ref}(T) = E_{Ref}^0(T) + r_f T \log_{10} a_{Cl^-, Ref}$  and  $E_{Ref}^0(T)$  was determined from an empirical equation [46].

<sup>b</sup> See Table 6.

<sup>c</sup> Slope of the linear regressions of experimental data in Fig. 6.

<sup>d</sup> Slope of the linear regressions of experimental data in Fig. 7.

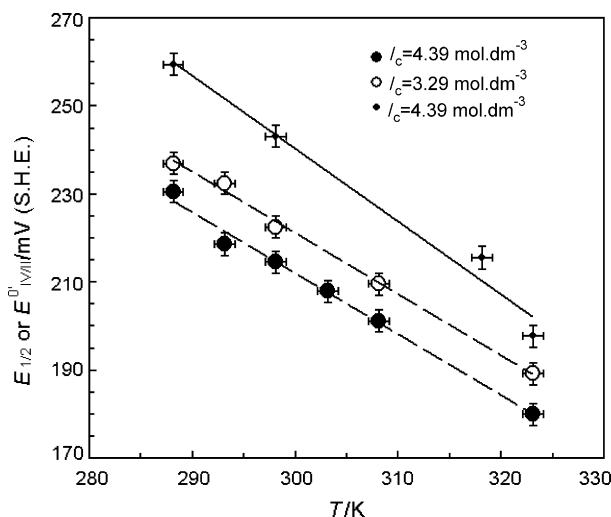


Fig. 6. Temperature influence on  $E_{1/2}(T)$  (black and hollow circles) and on  $E_{IV/III}^{0'}(T)$  (little black circles).

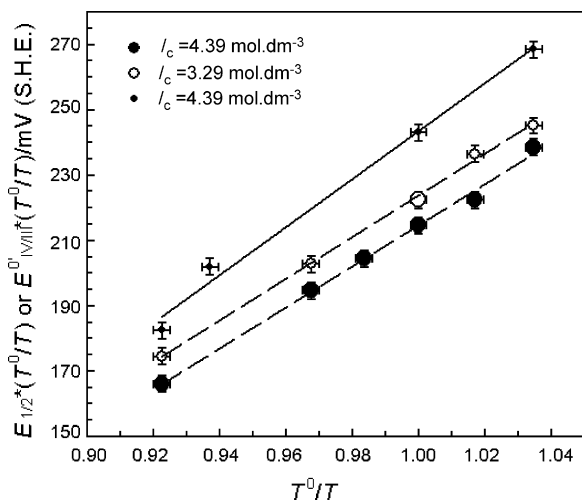


Fig. 7. Van't Hoff plot for  $E_{1/2}(T)$  (black and hollow circles) and  $E_{IV/III}^{0'}(T)$  (little black circles).

lines), according to Eq. (29), which becomes

$$\frac{E_{1/2}(T)T^0}{T} \approx \frac{\Delta_r S_{T^0} T^0}{F} - \frac{\Delta_r H_{T^0} T^0}{FT} \quad (35)$$

$\Delta_r S_{T^0}$  values are so verified by Eq. (35) and  $\Delta_r S_{T^0}$  and  $\Delta_r H_{T^0}$  values are given in Table 7. The  $\Delta_r G_{T^0}$  values determined from experimental data ( $E_{1/2}(T)$ ) and fitted data ( $E_{IV/III}^{0'}(T)$ ) are equal to  $-20 \text{ kJ mol}^{-1}$  and  $-24 \text{ kJ mol}^{-1}$ , respectively. The  $4 \text{ kJ mol}^{-1}$  in energy, corresponding to a  $40 \text{ mV}$  difference in potential, may be related the fact that the partial dissociation of Ce(IV) and Ce(III) limiting complexes was only considered in the fits leading to the determination of  $E_{IV/III}^{0'}(T)$ . Hardwick and Robertson [15] determined the thermodynamic quantities:  $\Delta_r S_{T^0} = 231 \text{ J mol}^{-1} \text{ K}^{-1}$  and  $\Delta_r H_{T^0} = 64.8 \text{ kJ mol}^{-1}$  relative to the hydrolysis reaction of Ce(IV) in perchloric acid solution.

### 5. Conclusions

Starting from the  $\text{Ce}(\text{CO}_3)_4^{5-}$  limiting complex, our SWV measurements of the Ce(IV)/Ce(III) redox couple in carbonate/bicarbonate solutions with high ionic strengths ( $3.29 \text{ mol dm}^{-3}$  at  $4.39 \text{ mol dm}^{-3}$ ) in the  $15\text{--}50 \text{ }^\circ\text{C}$  range enable us to validate the stoichiometry of the Ce(IV) limiting complex ( $\text{Ce}(\text{CO}_3)_6^{8-}$ ). Variations of  $E_{1/2}(T)$  versus  $\log_{10} m_{\text{CO}_3^{2-}}$  at ambient lead to  $E_{IV/III}^{0'}(T)$ ,  $K_{IV,6}$  values in accordance with those reported in the literature. Temperature has a small and linear –within uncertainties– influence on these values. This linearity was used to propose the corresponding numerical values for the thermodynamic data:  $\Delta_r S_{T^0} = -154 \text{ J mol}^{-1} \text{ K}^{-1}$  and  $\Delta_r H_{T^0} = -70 \text{ kJ mol}^{-1}$ . DCP, CV and SWV measurements allowed the determination of the apparent diffusion coefficient of Ce(IV). As the stoichiometries of the limiting complexes are established by different studies, they can be starting points to determine in further works the aqueous speciation of cerium in environmental conditions.

## Acknowledgement

We thank Dr. C. Moulin of CEA for stimulating conversation.

## References

- [1] I. Grenthe, A.V. Plyasunov, K. Spahiu, in: I. Grenthe, I. Puigdomenech (Eds.), *Modelling in Aquatic Chemistry*, OECD-NEA, Paris, 1997, p. 325.
- [2] I. Grenthe, J. Fuger, R.J.M. Konings, R.J. Lemire, A.B. Muller, C. Nguyen-Trung, H. Wanner, *NEA-TDB Chemical Thermodynamics of Uranium*, Elsevier, 1992, p.715.
- [3] R. Silva, G. Bidoglio, M. Rand, P. Robouch, H. Wanner, I. Puigdomenech, *NEA-TDB Chemical Thermodynamics of Americium*, Elsevier Science Publishers B.V., 1995, p. 374.
- [4] J.A. Rard, M. Rand, G. Anderegg, H. Wanner, *Chemical Thermodynamics of Technetium*, Elsevier B.V., Amsterdam, 1999, p. 544.
- [5] R. Lemire, J. Fuger, H. Nitsche, P. Potter, M. Rand, J. Rydberg, K. Saphu, J. Sullivan, W. Ullman, P. Vitorge, H. Wanner, *Chemical thermodynamics of Neptunium and Plutonium*, Elsevier B.V., Amsterdam, 2001, p. 845.
- [6] R. Guillaumont, T. Fanghänel, J. Fuger, I. Grenthe, V. Neck, D.A. Palmer, H. Rand, *Update on the Chemical Thermodynamics of Uranium, Neptunium, Plutonium, Americium and Technetium*, Elsevier B.V., Amsterdam, 2003, p. 919.
- [7] T. Vercouter, P. Vitorge, B. Amekraz, E. Giffaut, S. Hubert, C. Moulin, *Inorg. Chem.* 44 (2005) 5833.
- [8] T. Vercouter, P. Vitorge, N. Trigoulet, E. Giffaut, C. Moulin, *New J. Chem.* 29 (2005) 544.
- [9] J.Y. Bourges, B. Guillaume, G. Koehly, D.E. Hobart, J.R. Peterson, *Inorg. Chem.* 22 (1983) 1179.
- [10] C. Riglet-Martial, P. Vitorge, V. Calmon, *Radiochim. Acta* 82 (1998) 69.
- [11] D. Ferri, I. Grenthe, S. Hietanen, F. Salvatore, *Acta Chem. Scand.* A37 (1983) 359.
- [12] J. Dervin, J. Faucherre, *Bull. Soc. Chim.* 11 (1973) 2926.
- [13] J. Dervin, J. Faucherre, *Bull. Soc. Chim.* 11 (1973) 2930.
- [14] A. João, H. Burrows, L. Ramos, H. Teixeira, *J. Coord. Chem.* 59 (2006) 531.
- [15] T.J. Hardwick, E. Robertson, *Can. J. Chem.* 29 (1951) 818.
- [16] L. Ramaley, M.S. Krause Jr., *Anal. Chem.* 41 (1969) 1362.
- [17] J.J. O’Dea, J. Osteryoung, R.A. Osteryoung, *Anal. Chem.* 53 (1981) 695.
- [18] K. Aoki, K. Tokuda, H. Matzuda, J. Osteryoung, *J. Electroanal. Chem.* 207 (1986) 25.
- [19] K. Aoki, K. Maeda, J. Osteryoung, *J. Electroanal. Chem.* 272 (1989) 17.
- [20] B.A. Brookes, J.C. Ball, R.G. Compton, *J. Phys. Chem. B* 103 (1999) 5289.
- [21] M.M. El Belamachi, Ph.D. Thesis, Paris 6 University, Paris, France, 1996.
- [22] D. Krulic, N. Fatouros, M.M. El Belamachi, *J. Electroanal. Chem.* 33 (1995) 385.
- [23] N. Fatouros, D. Krulic, N. Larabi, *J. Electroanal. Chem.* 55 (2004) 568.
- [24] N. Fatouros, D. Krulic, *J. Electroanal. Chem.* 520 (2002) 1.
- [25] N. Fatouros, D. Krulic, J. Chevalet, *J. Electroanal. Chem.* 37 (1988) 247.
- [26] A.J. Bard, L.R. Faulkner, *Electrochimie: Principes, Méthodes et Applications*, Masson, Paris, 1983, pp. 241–258.
- [27] G. Biederman (Ed.), *Dahlem Workshop on the Nature of Seawater, Ionic Media, Dahlem Konferenzen*, Berlin, 1975, p. 339.
- [28] G. Biederman, in: E.A. Jenne, E. Rizzarrelli, V. Romano, S. Sammartano (Eds.), *Metal Complexes in Solution, Introduction to the Specific Interaction Theory with Emphasis on Chemical Equilibria*, Piccin, Padua, Italy, 1986, p. 303.
- [29] J.N. Brønsted, *J. Am. Chem. Soc.* 44 (1922) 877.
- [30] J.N. Brønsted, *J. Am. Chem. Soc.* 44 (1922) 938.
- [31] E.A. Guggenheim, *Philos. Mag.* 19 (1935) 588.
- [32] G. Scatchard, *Chem. Rev.* 19 (1936) 309.
- [33] E.A. Guggenheim, J.C. Turgeon, *Trans. Faraday Soc.* 51 (1955) 747.
- [34] E.A. Guggenheim, *Applications of Statistical Mechanics*, Clarendon Press, Oxford, 1966.
- [35] F. Salvatore, E. Vasca, *J. Coord. Chem.* 21 (1990) 237.
- [36] F. Crea, C. De Stefano, A. Gianguzza, D. Piazzese, S. Sammartano, *Talanta* 68 (2006) 1102.
- [37] C. De Stefano, D. Milea, A. Pettignano, S. Sammartano, *Biophysical Chemistry* 121 (2006) 121.
- [38] H. Capdevila, Ph.D. Thesis, Paris–Sud University, Paris, France, 1992.
- [39] H. Capdevila, P. Vitorge, *CEA-N-2762*, 1994.
- [40] N. Fatouros, D. Krulic, J. Chevalet, *J. Electroanal. Chem.* 135 (1994) 364.
- [41] N.N. Greenwood, A. Earnshaw, *Chemistry of the Elements*, Pergamon Press, 1984.
- [42] S. Cotton, *Lanthanides and Actinides*, Macmillan Physical Science Series, 1991.
- [43] L. Ciavatta, D. Ferri, I. Grenthe, F. Salvatore, K. Spahiu, *Inorg. Chem.* 22 (1983) 2088.
- [44] L.H. Delmau, P. Vitorge, H. Capdevila, *CEA-N-2807*, 1995.
- [45] J. Dervin, J. Faucherre, P. Herpin, S. Voliotis, *Bull. Soc. Chim.* 9–10 (1973) 2634.
- [46] A.J. Bard, R. Parsons, J. Jordan, *Standard Potential in Aqueous Solutions*, Dekker Marcel Inc., New York, 1985, p. 304.